Quantitative Analysis of Silicon Influence and Deformation Impact on the Mechanical and Corrosion Characteristics of Nickel Aluminium Bronze (NAB) Alloy

*[1,2]Isaac E. Dongo, [2] Joseph A. Omotoyinbo, [2]Akinlabi Oyetunji and [2]Oloruntoba T. Daniel
[1] Department of Materials and Metallurgical Engineering, Kogi State Polytechnic, Lokoja, Nigeria
[2] Department of Materials and Metallurgical Engineering, Federal University of Technology Akure, Ondo, Nigeria.
isaacdongo@gmail.com ; dongoenesi@kogistatepolytechnic.edu.ng

Received: 16-JAN-2024; Reviewed: 04-FEB-2024; Accepted: 14-FEB-2024
https://dx.doi.org/10.4314/fuoyejet.v9i1.18

ORIGINAL RESEARCH

Abstract— Nickel aluminum bronze (NAB) alloy has become increasingly popular due to its superior strength, corrosion resistance, and thermal properties. This study provides an in-depth analysis of the effect of silicon and deformation percentages on the mechanical and corrosion characteristics of NAB alloy, for marine and architectural applications. The research was carried out by systematically varying the silicon percentage (0-10%) while the percentage of deformation ranges from 0-10% at ambient temperature (32 °C), and subsequent changes in its mechanical properties and corrosion resistance were observed. Mechanical properties such as ultimate tensile strength, ductility, and hardness were evaluated using standard testing methods. The results indicated a significant correlation between the silicon percentage and the mechanical properties. Specifically, an increase in the silicon percentage was found to enhance the tensile strength from 190.7 MPa to 590.8 MPa, the ductility from 23.7% to 46.9% and the hardness from 130.5 HV to 262.4 HV values of the NAB alloy. The corrosion rate of 5.49 mm/a was obtained for the reference material containing 0% Si at 0% (X0-0) deformation, while the least corrosion rate of $9.8x10^{-5}$ mm/y was recorded for 2 wt. % Si at 10% deformation (X2-5). These findings have significant implications for the use of NAB alloy in marine and architectural applications. When the silicon percentage is optimized, the mechanical strength and corrosion resistance of the alloy are enhanced, thereby improving the durability and longevity of structures made from the developed NAB alloy
s

Keywords— Silicon, Deformation, Corrosion, and Hardness

1 INTRODUCTION

Nickel-Aluminum-Bronze (NAB), a copper-based alloy enriched with aluminum, iron, and nickel is renowned for its superior mechanical properties and remarkable corrosion resistance (Bohm *et al.,* 2016; Thossatheppitak *et al.,* 2014). The excellent mechanical and functional properties of copper and its alloys have made it attractive to industries for use in various fields of engineering applications. The surge in demand for copper-based alloys in the manufacturing of automotive components, electrical parts, valves, and fittings can be attributed to their exceptional properties. These include corrosion resistance, ductility, malleability, non-magnetism; wear resistance, and machinability, along with excellent thermal and electrical conductivities. Its extensive use also spans the marine and architectural sectors (Anantapong *et al.,* 2016; Dongo et al., 2023; Hussein *et al.,* 2015).

However, the performance of the NAB alloy can be significantly influenced by its composition, specifically the silicon percentage (Dongo *et al.,* 2023; Yao *et al.,* 2022). Mechanical properties such as tensile strength, and hardness which must withstand various stresses and ductility, strains are critical for materials used in marine and architectural structures (Hussein *et al.,* 2015).

Previous studies have suggested that the silicon variation in the NAB alloy may affect the properties, but a detailed understanding is still lacking (Nnakwo *et al.,* 2019). This paper presents a systematic investigation into how the variation of the silicon and deformation percentages alters the Mechanical properties of the NAB alloy. Through rigorous testing, we aim to establish a clear relationship between the silicon variation and the alloy tensile strength, ductility and hardness with respect to the deformation percentage.

Corrosion resistance is another crucial property for materials used in marine environments, where the presence of saltwater can lead to rapid degradation of materials (Poorjary *et al.,* 2023; Rivero *et al.,* 2021). The role of silicon in improving the corrosion resistance characterization of NAB alloy is a focus of ongoing research. In this study, we conducted a series of mechanical and electrochemical property tests to evaluate how silicon and deformation variations affect the resistance of the alloy to corrosion in a simulated marine environment.

2 METHODOLOGY

The primary constituents of the fabricated NAB alloy are copper, aluminum, nickel, manganese, zinc, and iron. Copper and aluminum are sourced from scrap materials such as refrigeration pipes, electrical motor engine coils, and aluminum tins. These materials are broken down into smaller pieces to expedite melting when placed in a

*Corresponding Author

Section B- MATERIALS/METALLURGICAL ENGINEERING AND RELATED SCIENCES

Can be cited as:

Dongo E.I., Omotoyinbo A.J., Oyetunji A. and Oloruntoba T.D. (2024): Quantitative Analysis of Silicon Influence and Deformation Impact on the Mechanical and Corrosion Characteristics of Nickel Aluminium Bronze (NAB) Alloy, FUOYE Journal of Engineering and Technology (FUOYE**JET), 9(1), 117-123. https://dx.doi.org/10.4314/fuoyejet.v9i1.18**

crucible pot within an oil-fired pit furnace. Silicon, magnesium, and iron are added in powdered form, stirred, and subsequently poured into pre-prepared mold cavities to create a 30 cm x 16 ϕ sample, which serves as the reference material for the study.

Six distinct composition samples, designated as X0, X1, X2, X3, X4, and X5, were sand-cast with varying weight percentages of silicon content at 0%, 2%, 4%, 6%, 8%, and 10% respectively (Table 1). Following post-casting and fettling operations, the materials were subjected to deformation (cold rolling) at ambient temperature (32 °C) at 0%, 2%, 4%, 6%, 8%, and 10% on each of the developed samples. This was then followed by stress-relief annealing at 450 °C for a holding time of 60 minutes, succeeded by slow cooling.

The resulting NAB alloy was then subjected to mechanical property tests and corrosion evaluation using Tafel potentiodynamic polarization (Dongo et al., 2023). Table 1 presents the analysis of the elemental compositions of the developed NAB alloy used as reference materials.

Table 1: Elemental Chemical Composition of the Developed NAB Alloy

Element	Sample X0	Sample X1	Sample X2	Sample X3	Sample X4	Sample X5
Cu	78.56	78.56	78.61	78.54	78.58	78.59
Al	10.85	10.83	10.92	10.91	10.86	10.83
Fe	3.09	3.09	3.10	3.09	3.10	3.09
Na	1.68	1.65	1.64	1.78	1.77	1.71
Ni	3.79	3.77	3.75	3.77	3.76	3.77
Si	0.00	0.16	0.32	0.48	0.64	0.80
Cl	0.24	0.21	0.21	0.25	0.22	0.27
Zn	0.57	0.59	0.58	0.59	0.58	0.58
S	0.08	0.08	0.05	0.04	0.07	0.07
Mg	0.25	0.24	0.25	0.25	0.25	0.24
P	0.05	0.06	0.07	0.06	0.08	0.05
Mn	0.34	0.35	0.35	0.32	0.34	0.32

3 Effect Of Silicon Variation On The Mechanical Properties Of Nab Alloy

The results suggest that a significant modification exists in the mechanical properties of the samples alloyed with silicon as compared to the unalloyed samples. The effect of Si on the hardness value ranges from 130.5 HV to 210.8 HV with it best hardness value at 8% Si variation (Figure 1), the strength ranges from 190.7 MPa to 405.6 MPa (Figure 2) and exhibits its highest strength value at 8% silicon variation, while the ductility ranges from 23.7% to 39.9%. The results generally show that silicon addition beyond 8% does not have any positive impact on the developed NAB alloy.

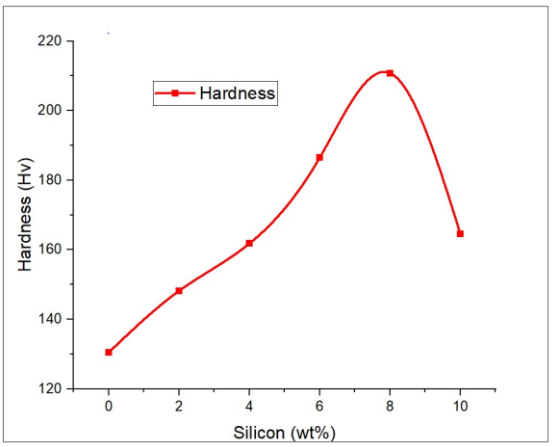

Figure 1: Relationship between Hardness and Si Ratio

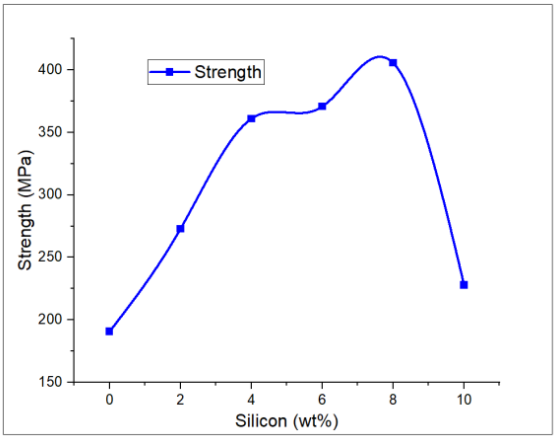

Figure 2: Relationship between Tensile Strength and Si Percentage

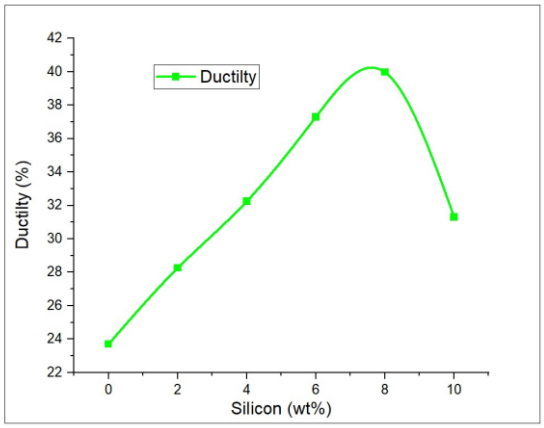

Figure 3: Relationship between Ductility and Si Percentage

3.1 Effect of Silicon and Deformation Percentage on the Mechanical Properties of NAB Alloy

It was apparent that further increase in the hardness, Strength, and ductility value is associated to deformation percentages of the cast samples, this values range from 130.5 HV to 262.4 HV for hardness (Figure 4), while 190.7 MPa to 590.8 MPa was recorded for the

strength (Figure 5) and the ductility ranging from 23.7% to 46.9% with respect to deformation percentage.

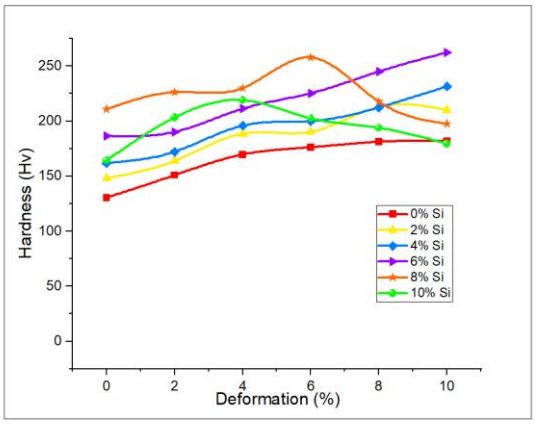

Figure 4: Relationship between Hardness and

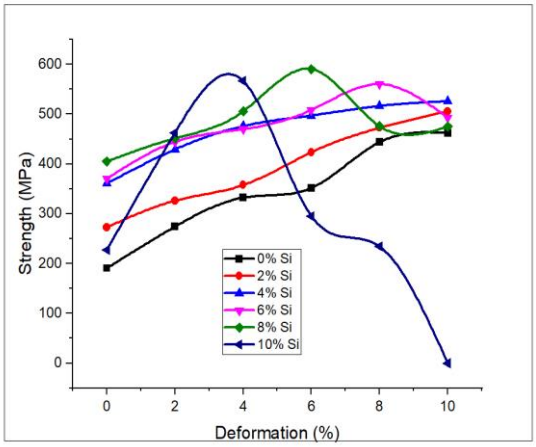

Figure 5: Relationship between Tensile Strength and

3.2. Influence of Silicon Percentage on the Microstructure of NAB alloy

The microstructure of the alloy was found to contain a considerable volume of cells and cavities present in the grains and act as obstacles to the motion of dislocation resulting into increase in hardness of the developed alloy. Plates 1a to 6a show the microstructural images of the alloy with different percentages of silicon content.

Plate 1: Optical Micrograph of as Received Sample at 0% Deformation (X0-0)

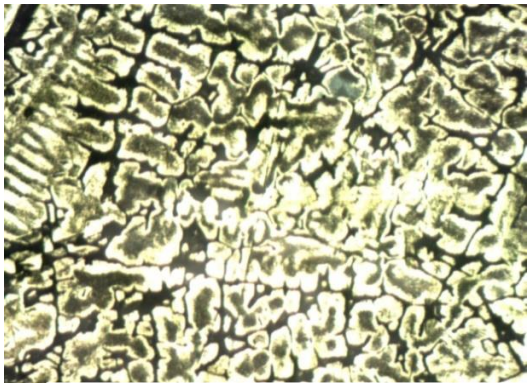

Plate 2a: Optical Micrograph of Sample of 2% Si at 0% Deformation (X1-0)

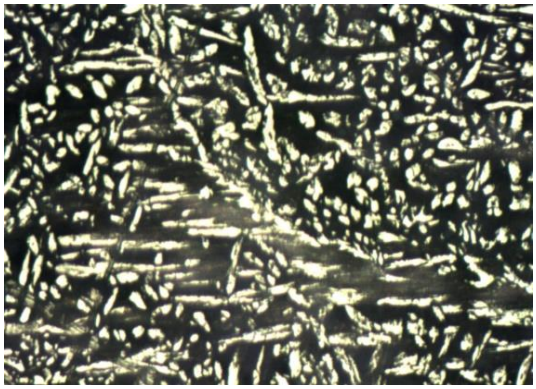

Plate 3: Optical Micrograph of Sample of 4% Si at 0% Deformation (X2-0)

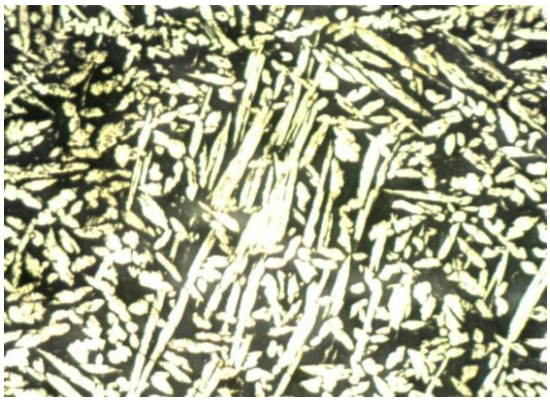

Plate 4: Optical Micrograph of Sample of 6% Si at 0% Deformation (X3-0)

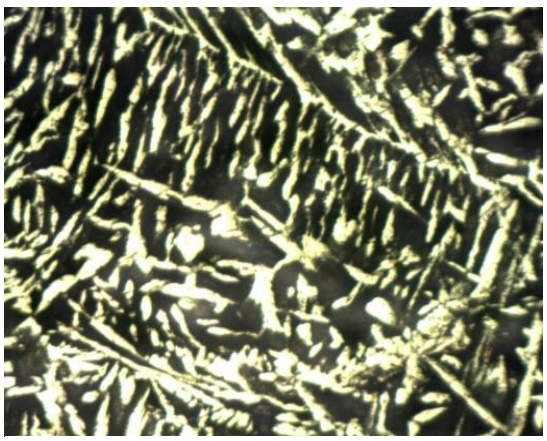

Plate 5: Optical Micrograph of Sample of 8% Si at 0% Deformation (X4-0)

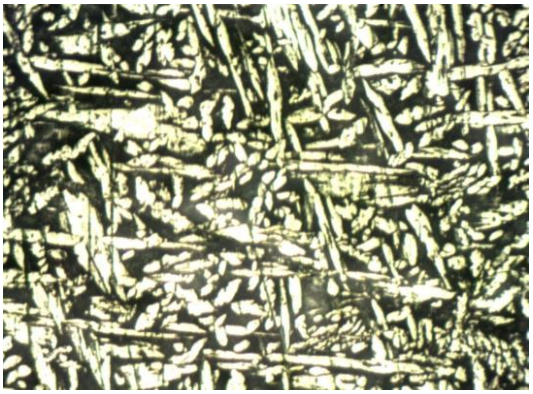

Plate 6: Optical Micrograph of Sample of 10% Si at 0% Deformation (X5-0)

Plates 1 – 6 show the microstructure of the developed NAB alloy with respect to increase in the weight percentage of silicon. In general, as the silicon content increases, the average grain size also increases. The microstructure also becomes less uniform, with more variation in grain size and shape. The presence of kappa phases also increases as the silicon content increases. In terms of performance, the developed NAB alloy is at its best when it has a moderate amount of kappa phases, typically around 6% to 8% by volume (plates 4 and 5 respectively). This gives a good balance of strength, hardness, and ductility. Usually alloys with a very high or very low amount of kappa phases tend to be less useful, since they do not have the right balance of properties.

The increased amount of kappa phases, as the silicon content increases, has a few different effects. First, the alloy becomes more resistant to corrosion. Second, the alloy becomes stronger and harder. Third, the alloy becomes more ductile, which means that it can be stretched or bent without breaking. These changes are beneficial, and they make the NAB alloy more suitable for a variety of applications.

3.3. Examining the Impact of Silicon and Deformation on the Corrosion Characteristics of NAB Alloy

The Electrochemical Corrosion Potential (Ecor) and Corrosion Current Density (icor) are both related to the corrosion rate, but they provide additional information as well. Ecor indicates the material's tendency to corrode, while icor provides information about the actual rate of corrosion. The potentio-dynamic curves for the unreinforced samples (0 wt. % Si) were observed to display corrosion potential values of -0.28728 V at a corrosion rate of 5.4962 mm/y (Figure 5a). However, as the samples underwent deformation (2%, 4%, 6%, 8%, and 10%), they displayed increasing corrosion potential values of -0.2895 VAg/AgCl, -0.30162 VAg/AgCl, -0.30705 VAg/AgCl, -0.2852 VAg/AgCl, and -0.23826 VAg/AgCl, respectively.

Similar trends were observed for samples with varied weight percentages of Si reinforcement, with the reference samples displaying the highest corrosion rate. As the materials were subjected to deformation, the corrosion rate reduced from 5.4962 mm/y to -0.00049247 mm/y. The results indicate that as deformation increases, the corrosion rate decreases, suggesting a reduced tendency for corrosion with increased deformation. As for the icor values, they also decreased as the deformation increased, from 0.00047 A/cm^2 at 0% deformation to -4.2195 $\times 10^8$ A/cm^2 at 10% deformation. This suggests that the rate of corrosion decreases as the deformation increases.

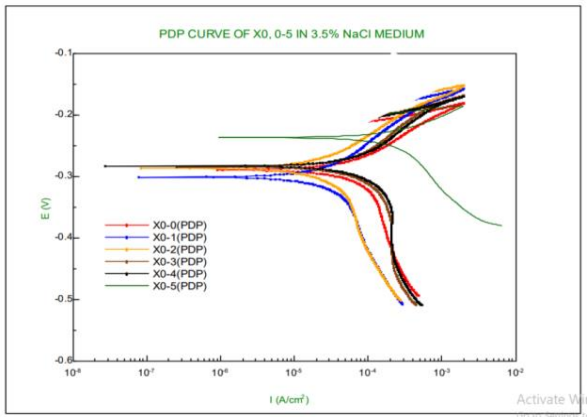

Figure 5a: Potentiodynamic polarization curves of 0% Si

In Figure 5b, Sample $X_{1\text{-}0}$ exhibits the lowest corrosion potentials of -0.36406 VAg/AgCl and the highest corrosion rate of 1.3274 mm/y in that series. All deformed samples display improved corrosion resistance to their respective degree of deformation in this series. It was observed that sample $X_{1\text{-}5}$ displayed the highest value (-9.87x10^{-5} mm/y) corrosion susceptibility in the X1 sample series.

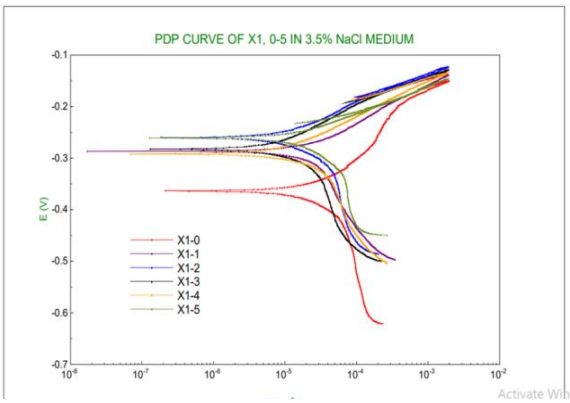

Figure 5b: Potentiodynamic polarization curves of 2% Si

The trend depicted in Figure 5c shows that sample X2-0 exhibited the least susceptibility to corrosion, at a rate of 0.76759 mm/y. This is in contrast to sample X2-5, which displayed an optimal value of 0.0046757 mm/y in the X2 series when subjected to deformation. It was observed that the Ecor values increased with the effect of silicon as the deformation increased. Simultaneously, there was a decrease in the icor values as the deformation increased, leading to a decrease in the corrosion rate.

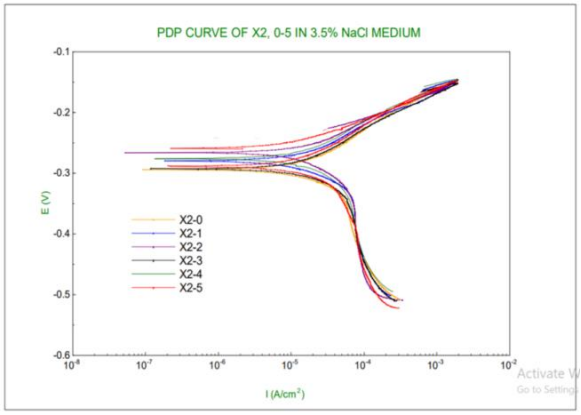

Figure 5c: Potentiodynamic polarization curves of 4% Si

Based on this trend, we can conclude that the material becomes more resistant to corrosion as the deformation ratio increases in relation to the silicon ratio. It's possible that as the material deforms, it becomes more compact and has fewer defects. This makes it more difficult for corrosive agents to penetrate the material, resulting in a decrease in the corrosion rate. Additionally, the deformation process could potentially lead to the formation of a passive layer on the surface of the material, which could enhance its resistance to corrosion.

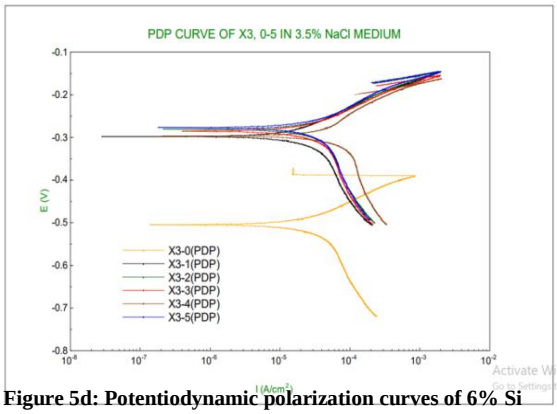

Figure 5d: Potentiodynamic polarization curves of 6% Si

The results presented in Figure 5d reveal a marked increase in the corrosion rate of the reference sample compared to others, thereby demonstrating the beneficial influence of Si in enhancing the corrosion properties of the developed material. From the results, it can be inferred that sample X3-3 exhibits an optimal corrosion resistance value of -22162 mm/y and a corrosion potential of -23550 V in a saline environment. When considering the data for sample X3, the corrosion rate was observed to decrease by approximately 2% in the deformation ratio. However, it begins to increase again at a deformation ratio of around 6%. This behavior could be attributed to the formation or breakdown of the oxide layer that serves as a protective layer on the surface of the sample.

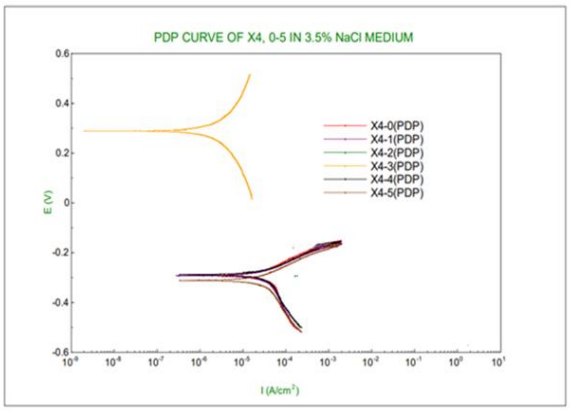

Figure 5e: Potentiodynamic polarization curves of 8% Si

As depicted in Figure 5e, the corrosion rate initially decreases as the amount of deformation increases, but then it starts to increase at higher levels of deformation. Interestingly, the corrosion rate peaks at 8% deformation, suggesting that the alloy becomes more prone to corrosion beyond this point.

The Ecor values increase from -0.29282 VAg/AgCl to -0.28486 VAg/AgCl, and the icor values decrease from 0.89527 A/cm² to -0.000060288 A/cm² as the deformation level increases from 0% to 6%. However, beyond this point, both the Ecor and icor values start to increase. The Ecor values rise from -0.28486 VAg/AgCl to -0.3206 VAg/AgCl, and the icor values increases from -0.000060288 A/cm² to -0.03329 A/cm² as the deformation level increases from 6% to 10%.

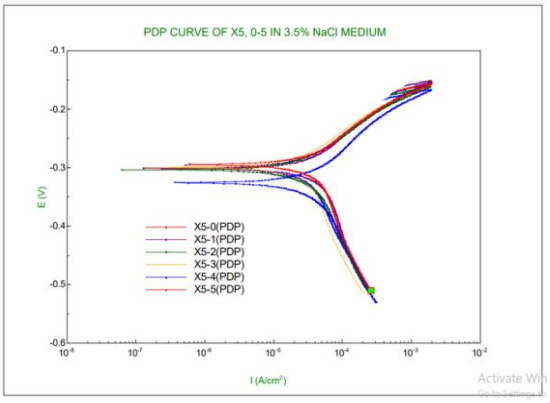

Figure: 5f: Potentiodynamic polarization curves of 10% Si

This indicates an improvement in resistant to corrosion as the deformation level increases beyond 6%. The results suggest that there exists an optimal level of deformation for this alloy, at which the corrosion resistance is at its peak. However, any further deformation beyond this point leads to a decrease in corrosion resistance, and ultimately, the failure of the alloy.

These findings are crucial when designing applications for this alloy, as they ensure its usage in a manner that optimizes its corrosion resistance and extends its lifespan. It's important to note that the corrosion resistance of this alloy is just one of many factors to consider during the design process. Other factors such as strength, toughness, and cost must also be taken into account.

Sample $X_{5\text{-}0}$ suggests that the unreformed recorded the highest corrosion rate of 3.429 mm/y in this series, while sample $X_{5\text{-}2}$ recorded the optimal corrosion resistance of 0.17466 mm/y in the 3.5% NaCl solution (Figure 5f). The observed reduction in the corrosion resistance beyond the 4% deformation ratio is perhaps due to the aggressiveness of the corrosion medium, which in turn led to the formation of film on the surface of the sample when in the NaCl solution environment.

The Ecor and icor values appear to have an inverse relationship with the corrosion rate. As the Ecor value increases, indicating a lower tendency for the metal to corrode, the corrosion rate decreases. Conversely, as the icor value increases, reflecting a higher rate of corrosion, the corrosion rate also increases. This is consistent with the established theory of corrosion. In summary, while Ecor values are inversely related to the corrosion rate, icor values are directly related to it.

In general, the addition of silicon and the deformation ratio to the developed samples reduce the alloy's susceptibility to corrosion when exposed to a 3.5% NaCl medium. All reference samples are more prone to corrosion prior to undergoing deformation. The results show a decrease in the corrosion rate for samples alloyed with 2 wt.% and 4 wt.% Si addition over the deformation ratio, compared to the sample without Si addition and deformation (X0-0). However, a sharp increase in the corrosion rate was observed for samples with silicon additions between 6 wt.% and 8 wt.% over the deformation ratio. This could be attributed to the aggressiveness of the corrosion medium (Oluyori et al., 2017).

It was observed that the corrosion of silicon reinforcement in steel initially decreases in a NaCl solution, but later increases due to the aggressiveness of the corrosion medium. There is also evidence suggesting that silicon affects the structure and composition of the oxide layer on the surface of alloys. For instance, silicon has been shown to increase the density of the oxide layer, potentially enhancing its resistance to corrosion (Deevi et al., 2010).

4 CONCLUSIONS

The study recognizes that the optimal silicon ratio may differ based on the unique requirements of each application. Overall, this research enriches the existing knowledge on NAB alloys and provides valuable insights for industries engaged in marine and architectural design. It emphasizes the importance of comprehending the material properties of alloys and their reactions to various environmental conditions for making informed decisions in material selection and design. However, the study concludes as follows:

- The study found that both the micro-hardness and tensile strength of the alloy significantly improved with an increase in deformation and silicon addition. Through a combination of microscopic mechanical testing and microstructural characterization, it was shown that the micro-hardness properties of the alloy were strongly dependent on the silicon content and deformation ratio.
- The study found that a positive corrosion potential of 0.28746 VAg/AgCl was achieved with 8% silicon and 8% deformation ratios. However, the lowest corrosion rate of $9.87x10^{-5}$ mm/y was observed for a sample deformed at 10% with a 2% silicon addition. These results suggest a relationship between deformation and corrosion, which could be beneficial in the development of new materials with enhanced corrosion resistance.

ACKNOWLEDGEMENT

The Authors wish to express their appreciation to the Tertiary Education Trust Fund (Tetfund) for sponsoring the project. Our profound gratitude also goes to Engr. Dr. & Mrs. Amoka, S. Irimya, The Executive Director of EchoGems Consult Ltd, Kaduna State. Additionally, We are immensely grateful to the family of Mr. & Mrs. Madukwe Chinedu for their substantial contributions and encouragement.

REFERENCES

Anantapong, J., Uthaisangsuk, V., Suranuntchai, S. & Manonukul, A.(2014). Effect of hot working on microstructure evolution of as-cast nickel-aluminum –bronze alloy. *Materials and Design*, 60, Pp. 233-243. https://doi.org/10.1016/j.matdes.2014.03.033

Bohm, J., Linhardt, P., Strobl, S., Haubner, R. & Beizm, M. V. (2016). Microstructure of a heat treated Nickel-aluminium-bronze and its corrosion behavior in simulated fresh and seawater. *Materials Performance and Characterization*, 5(5), Pp.689-700. https://doi.org/10.1520/MPC20160029.

Deevi, S. K., Singj, K. P. & Zaki, M. I. (2010). Effect of Silicon on the

Microstructure and Corrosion Behaviour of Nitrided Ferritic Stainless Steel. *Corrosion Science*, Vol.52, No.3,Pp. 1142-1152

Ding, D., Zengxi P., Stephen Van Duin, Huijun Li, and Chen Shen. (2016). Fabricating Superior NiAl Bronze Components through Wire Arc Additive Manufacturing, *Materials* 9, no. 8: 652. https://doi.org/10.3390/ma9080652

Dongo, E. I., Omotoyinbo, J. A., Oyetunji, A. & Oloruntoba, D. T. (2023). Effects of Silicon and Deformation Ratio on the Mechanical Behaviour of Nickel Aluminum Broze (NAB) Alloy. X(2321), Pp 241-247. https://doi.org/10.51244/IJRSI

Hebda, M., Debecka, H. & Kazior, J. (2015). Influence of Silicon Addition on the Mechanical Properties and Corrosion Resistance of low-alloy Steel. *Bulletin of Materials Science*, 38, Pp. 1687-16921

Han, X. (2022) The Laser deposited Nickel-aluminm-bronze alloy. Metals, 12(5), 781

Hussein, A. A., Banna, E. M. & Waly, M. A. (2015). Effects of Chromium and Silicon Additions on the Microstructure and Mechanical Properties of Complex Aluminum Bronze, 5(2). Pp. 17-22.

Nnakwo, K. C. & Nnuka, E. E. (2018). Correlation of the Structure, Mechanical and physical Properties of Cu-3wt.% Si-xwt.% Sn Silicon Bronze. *Journal of Engineering and Applied Sciences*, 13, Pp. 83-91

Oluyori, T., Olorunniwo, O.E., & Fayomi, O. S. I. (2017). Performance Evalution Effect of Nb2O5 Particulate on the Microstructural, Wear and Ti-Corrosion Resistance of Zn-Nb2O5 Coatings on the Mild Steel for Marine Application. Journal of Bio-Tribo Corrossion 3, 51. https://doi.org/10.1007/s40735-017-0108-x

Poorjary, S., Marakini, V., Rao, R. N. & Vijayan, V. (2023). Enhancing Microstructure and Mechanical Properties of Nickel Aluminum Bronze Alloy Through Ti Addition. Scientific Reports, 13(1), 1-8, https://doi.org/10.1038/s41598-023-44146-y

Rivero, P., Berlanga, C., Palacio, J. F., & Biezma-Moraleda, M. V. (2021). Effect of Ti on Microstructure, Mechanical Properties and Corrosion Behavior of a Nickel Aluminum Bronze Alloy. Materials Research. 24(2). https://doi.org/10.1590/1980-5373-MR-2020-0335

Thossatheppitak, B., Suranuntchai, S. Uthaisangsuk, V., Manonukul, A., & Mungsuntisuk, P. (2014). Microstructure Evolution pf Nickel Aluminum Broze Alloy During Compression at Elevated Temperatures. Advanced Materials Research. 893, Pp. 365-370 https://doi.org/10.4028/www.science.net/AMR.893.365

Yao, C. L., Kang, H. S., Lee, K. Y., Zhai, J. G., & Shim, D. S. (2022). A Study on mechanical Properties of CuNi2SiCr Layered on Nickel Aluminum Bronze via Directed Energy Deposition. Journal of Materials Research and Technology, 18, 5337-5361. https://doi.org/10.1016/j.jmrt.2022.04.159